RSC Advances

ROYAL SOCIETY OF CHEMISTRY

www.rsc.org/advances

Polyiminofluorene with Conjugated Benzimidazolylpyridine Substituent Groups: Optical Properties, Ionochromism and Coordinative Self-Assembly into Electrochromic Films

Kalie Cheng and Bernd Tieke*

Department of Chemistry
University of Cologne
Luxemburger Str. 116
D-50939 Cologne
Germany

---

*) author to whom correspondence should be addressed; tieke@uni-koeln.de

Abstract

Synthesis and characteristic properties of polyiminofluorene **P1** with 2,6-bis(1‘-methylbenzimidazolyl)pyridine (bip) ligands attached to the N-atoms of the backbone via conjugated 4-ethinylenephenylene spacer units are reported. **P1** was obtained upon Pd-catalyzed amination of 2,7-dibromo-9,9-dihexylfluorene with 4-(2-(2,6-bis(1‘-methylbenzimidazolyl)pyridinyl)-ethinyl)aniline. MALDI-TOF spectrometry shows that oligomers up to the tetradecamer are formed, the hexamer being the most abundant species. **P1** is soluble in organic solvents such as xylene, toluene, or chlorobenzene forming yellow solutions with blue, green or yellow fluorescence depending on the polarity of the solvent. The fluorescence quantum yield in xylene is 41%. UV/Vis titration of the polymer with zinc chloride in toluene/methanol (49:1) indicates formation of 2:1 ligand:metal (bis) complexes and 1:1 mono complexes. Complex formation with various divalent transition metal ions is accompanied with ion specific colour changes (ionochromism) and quenching of the polymer fluorescence. The coordinative interactions between the bip ligands and metal ions such as Zn(II) or Cu(II) has been used for layer-by-layer assembly of ultrathin films on solid supports. Sequential adsorption of metal ions and **P1** leads to formation of ultrathin coordination polymer networks films. Due to ion specific metal-to-ligand charge transfer the **P1**/Zn(II) films are orange, while **P1**/Cu(II) films are purple. If anodically oxidized up to 750 mV vs. FOC, **P1**/Zn(II) and **P1**/Cu(II) films change colour into blue due to oxidation of the polymer backbone. Colour changes are reversible. Films prepared upon 12 dipping cycles exhibit switching times from the neutral to the oxidized state of 300 to 500 ms, the contrast beeing up to 53%. SEM studies indicate a homogeneous surface, which becomes slightly inhomogeneous after electrochemical cycling.

1. Introduction

Coordinative self assembly of organic compounds and inorganic transition metal salts has been proven to be a suitable method for preparation of coordination polymers with interesting materials properties.[1-8] Photo- and electroluminescent,[9] electrochromic,[10,11] and photovoltaic polymers can be prepared.[12] If carried out on a solid substrate in a step-by-step approach, alternating self-assembly of organic and inorganic compounds can be used to build up films of coordination polymers with precisely controlled thickness in the nanometer range.[13,14] Several examples of multiple sequential assembly of ditopic organic ligands and transition metal salts have been reported to result in functional films useful in electronics, optoelectronics, or as sensors.[13,15-17]

Recent studies have demonstrated that the use of oligo- or polytopic ligands is a promising alternative to ditopic ligands.[18,19] Ditopic ligands exhibit some disadvantages, e.g., they are easily desorbed from the substrate, sometimes tend to crystallize, and do not allow for healing of defects during the layer-by-layer deposition of ultrathin films. Alternating assembly of metal salts and polymers with ligand groups attached to the backbone, so-called polytopic ligands, is better suited, because stable films of coordination polymer networks well-adhering to the surface are obtained (Scheme 1). Using this approach electrochromic and photoluminescent films were recently described.[20,21] It was shown that a structural variation of the polymer,[22] the metal ions,[22] and counterions[23] can be used to tune-up and optimize the optical and electronic properties of the films.

Up to now mainly polymers substituted with terpyridine (tpy) ligands were used for preparation of electrochromic films. Only one example of a polymer with 2,6-bis(1‘-

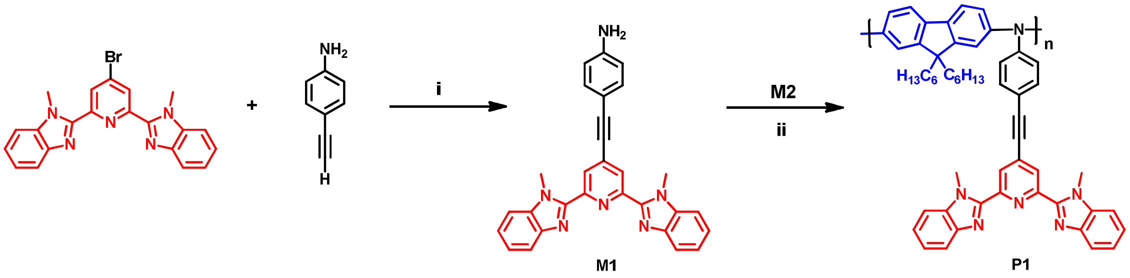

Scheme 1: Preparation of monomer **M1** and polymer **P1**. (**i**) Pd(PPh$_3$)$_2$Cl$_2$, CuI, TEA, 3.5 h in DMF at 90 °C; (**ii**) Pd$_2$(dba)$_3$, P^t(Bu)$_3$, NaO^{t}Bu, 16 h in toluene at 100 °C.

methylbenzimidazolyl)pyridine (bip) ligands attached to the conjugated main chain via alkylene spacer units has been reported up to the present.[21] While the preparation of tpy ligands is rather time-consuming and costly, bip ligands can be synthesized more easily on a large scale.[25] Therefore it was of interest to prepare a new polytopic ligand consisting of a conjugated main chain and conjugated bip units attached to it. Since we were interested in electrochromic films we prepared **P1** (Scheme 1) with easily oxydizable iminofluorene backbone and bip units attached to the N-atoms of the backbone via conjugated spacer units. **P1** was synthesized upon palladium-catalyzed coupling of 2,7-dibromo-9,9-dihexylfluorene and 4-ethinylaniline comonomers.[26-28,30.]

In our contribution, preparation and characteristic properties of **P1** are reported, as well as studies of metal ion complexation, ionochromism, coordinative layer-by-layer (lbl) assembly into ultra thin films, and electrochromic properties of the films. Analytical studies were carried out using spectroscopic and microscopic methods such as NMR, UV and fluorescence spectroscopy, SEM, and cyclic voltammetry. It is demonstrated that **P1** is an interesting new material suitable for metal ion complexation and sensing, and for preparation of ultrathin electrochromic films via coordinative self-assembly.

2. Experimental part

2.1 Materials.

Copper chloride dihydrate ($CuCl_2 \cdot 2H_2O$), iron(III) chloride hexahydrate ($FeCl_3 \cdot 6H_2O$), iron(II) perchlorate hydrate($Fe(ClO_4)_2 \cdot xH_2O$) and zinc chloride ($ZnCl_2$) were obtained from Acros. Manganese(II) chloride tetrahydrate ($MnCl_2 \cdot 4H_2O$) and cobalt chloride hexahydrate ($CoCl_2 \cdot 6H_2O$) were obtained from Merck. Nickel chloride hexahydrate ($NiCl_2 \cdot 6H_2O$) was obtained from Fluka. Dithranole, silver tetrafluoroborate ($AgBF_4$), phosphorus(V) oxybromide ($OPBr_3$) and potassium hexafluorophosphate (KPF_6) were obtained from Aldrich. All salts were used without further purification. The solvents were obtained from Aldrich with high purity grade and used without further purification. Milli-Q water was used for all experiments. 2,6-Bis-(1‘-methylbenzimidazolyl)-4-hydroxypyridine (**1**) and 2,7-dibromo-9,9-dihexylfluorene (**M2**) were prepared according to the literature.[31,32]

2.2 Synthesis.

2.2.1 Synthesis of 2,6-bis(1‘-methylbenzimidazolyl)-4-bromopyridine (2).

647 mg (1.82 mmol, 1 eq.) 2,6-Bis-(1‘-methylbenzimidazolyl)-4-hydroxy-pyridine[31] (**1**) were dissolved in 6.47 g (22.8 mmol, 12.5 eq.) of molten phosphorus(V) oxybromide ($OPBr_3$) at 70 °C. The reaction mixture was stirred at 140 °C under inert conditions for 16 h. After cooling to room temperature 40 ml of Milli-Q water were added to the reaction mixture. Then the mixture was stirred at 80 °C for 1 h. A solution of 1 M NaOH in water was added until the mixture was alkaline. The precipitate was filtered, washed with Milli-Q water and dried in vacuo to yield 769 mg of a white powder. Yield: 98 %, m.p.: >290 °C.

^{1}H-NMR (DMSO-d^6, 300 MHz): δ (ppm) 4.31 (s, methyl, 6H); 7.53 (m, phenylene, 4H); 7.9 (dd, phenylene, 4H); 8.7 (s, pyridine, 2H).

2.2.2 Synthesis of 4-(2-(2,6-bis(1‘-methylbenzimidazolyl)pyridinyl)-ethinyl)aniline (M1).

Under inert conditions 257.3 mg (2.20 mmol, 1.3 eq.) 4-ethinylaniline, 39.1 mg (3.3 mol %) bis(triphenylphosphine)palladium(II) chloride, and 12.9 mg (4.0 mol %) copper(I) iodide were dissolved in 14 ml degassed triethylamine (TEA). 707 mg (1.69 mmol, 1 eq.) 2,6-Bis(1‘-methylbenzimidazolyl)-4-bromopyridine (**2**), dissolved in 4 ml degassed DMF, were added to the solution and the reaction mixture was stirred at 90 °C for 3.5 h. Then the mixture was poured in 300 ml Milli-Q water, and the monomer precipitated. The product was filtered and washed with water. The raw product was recrystallized from dichloromethane (DCM)/diethylether (volume ratio: 1:2) to yield 660 mg of the clean product. Yield: 86 %, m.p.: >290 °C.

^{1}H-NMR (DMSO-d^6, 300 MHz): δ (ppm) 4.29 (s, methyl, 6H); 5.86 (s, amine, 2H); 6.62 (d, aniline, 2H); 7.37 (m, phenylene, 4H); 7.40 (d, aniline, 2H); 7.75 (dd, phenylene, 4H); 8.35 (s, pyridine, 2H).

UV (DMSO): 353 nm; $\varepsilon_{(353\ \mathrm{nm})}$ = 8636 L mol^{-1} cm^{-1}. PL$_{(\mathrm{toluene})}$: 453 nm, excitation at 353 nm.

2.2.3 Synthesis of P1.

Under inert conditions 215.8 mg (0.44 mmol, 1 eq.) 2,7-dibromo-9,9-dihexylfluorene (**M2**), 128 mg (1.33 mmol, 3 eq.) sodium *tert*-butoxide, 200 mg **M1** (0.44 mmol, 1 eq.) and 15 ml of degassed toluene were charged in a Schlenk tube. The catalyst was prepared by stirring a mixture of 10.1 mg (2.5 mol %) $Pd_2(dba)_3$ and 13.4 mg (15 mol %) tri-*tert*-butylphosphine in

4 ml toluene under inert conditions for 30 min. After addition of the catalyst solution the reaction mixture was stirred at 100 °C for 16 h. Then the mixture was cooled to room temperature and quenched upon addition of 2 ml aqueous ammonia solution. The organic phase was washed several times with a saturated aqueous NaCl-solution, concentrated in vacuo and precipitated in methanol to yield 197 mg of the polymer as a yellow powder. Yield: 57 %.

^{1}H-NMR ($CHCl_3$-d^1, 300 MHz): δ (ppm) 0.4-2.0 (alkyl chain, 26H); 4.27 (s, methyl, 6H); 7.14 (d, aniline, 2H) 7.3 (m, phenylene, 4H); 7.37 (m, phenylene, 4H); 7,55 (d, phenyl-H, 2H); 7,75 (dd, phenyl-H, 4H); 7.91 (d, aniline, 2H), 8.53 (s, pyridine, 2H).

$UV_{(toluene)}$: 320 nm, 357 nm, 415 nm; $\varepsilon_{(353\ nm)}$ = 15354 L mol^{-1} cm^{-1}. $PL_{(toluene)}$: 496 nm, excitation at 357 nm.

2.3 Substrates.

Quartz substrates (size 30x12x1 mm^3) were cleaned upon immersion in a 7:3 mixture of 98% H_2SO_4 and 30% H_2O_2 7:3 for 1 h (***caution:** the mixture is strongly oxidizing and may detonate upon contact with organic material*). After multiple washing with Milli-Q water, the substrates were subjected to ultrasonication in alkaline isopropanol at 60 °C. Then the substrates were silanized with 3-aminopropyl(diethoxy)methylsilane (5%) in toluene, and finally precoated with three layer pairs of polystyrenesulfonate (PSS) and polyethyleneimine (PEI) as described in the literature.[33] The precoating was completed with a layer of PSS. Indium tin oxide (ITO) coated glass substrates were cleaned by subjecting the substrates to ultrasonication in a mixture of water and ethanol (1:1) for 30 min each. Subsequently the substrates were precoated with three layer pairs of (PSS) and (PEI).

2.4 Film preparation.

The multilayers were deposited on quartz and ITO substrates using multiple sequential coordinative layer-by-layer assembly. The precoated substrates were alternately dipped into solutions of the transition metal salts and **P1**. Solutions of $5 \cdot 10^{-3}$ M metal hexafluorophosphates in toluene/methanol (2:3) and a solution of $8.5 \cdot 10^{-5}$ M **P1** in toluene/methanol (2:3) were used for the film preparation. The metal hexafluorophosphate solutions were prepared by adding 2 eq. of potassium hexafluorophosphate in 1 ml DMF to the $5 \cdot 10^{-3}$ M solution of the corresponding metal chloride in toluene/methanol (2:3). After each dipping step the substrates were cleaned upon immersion in the pure toluene/methanol (2:3) solvent mixture.

2.5 Instrumentation.

UV-Vis-spectra were measured on a Perkin-Elmer Lambda 14 spectrometer. The baseline was corrected by subtracting the spectrum of a quartz substrate precoated with 3 layer pairs of PEI and PSS. Photoluminescence spectra were recorded on a Perkin-Elmer LS 50 B spectrometer. Photoluminescence quantum yields were measured in xylene, toluene and chlorobenzene solutions. The values were calculated by comparing with rhodamin 6G in ethanol ($\phi_R = 0.95$). MALDI-TOF experiments were carried out on a Bruker Daltonics Autoflex spectrometer. A dithranole matrix was used to which silver tetrafluoroborate was added. Cyclovoltammetric studies were carried out on a HEKA PG 390 potentiostat using Potpulse-software for data acquisition and potentiostat control. The experiments were carried out in a conventional three-electrode electrochemical cell at room temperature. Polymer coated ITO-substrates were used as working electrodes, platinum was used as counter and reference electrodes. A 0.1 M tetrabutylammonium hexafluorophosphate solution in acetonitrile saturated with nitrogen was used as electrolyte medium. SEM images were obtained using a Zeiss Neon 40 scanning electron microscope. EDX measurements were carried out on an INCA Drycool device connected to a Zeiss Neon 40 SEM. The images were obtained with an acceleration voltage of 20 kV over an area of 2500 µm^2. The film thickness was measured using a Vecco DekTak3. Multilayer films on quartz substrates were partially scratched from the substrate. The height profile was scanned with an error of ± 2.5 nm.

3. Results and discussion

3.1 Preparation of P1.

P1 was synthesized upon palladium-catalyzed Buchwald-Hartwig polycondensation of 2,7-dibromo-9,9-dihexylfluorene (**M2**) and **M1**. **M1** was obtained via Sonogashira-coupling of 4-ethinylaniline **(3)** and **2**. **2** was synthesized upon bromination of **1**, whereas **1** was obtained via a well known condensation reaction of chelidamic acid with N-methyl-phenylene-2,3-diamine.[31] $Pd_2(dba)_3$/tri-*tert*-butylphosphine was used as catalyst for polymerization, and sodium *t*-butoxide was used as base. The product was obtained as a yellow powder, which was soluble in common organic solvents like toluene, THF or DCM. The molecular weight distribution of **P1** was determined using MALDI-TOF spectrometry. The spectrum is shown in the Supporting Information (Fig. S1). A distribution of the absolute molecular weights of the different chain lengths was obtained. The assigned molecular weights correspond to exact multiples of the repeat unit of 785 *m/z*. The intense peak of 6 repeat units represents the most abundant chain length indicating that **P1** is actually an oligomer. A maximum of 14 repeat units could be detected. Fig. 1 shows the UV-Vis absorption spectrum of **P1** in toluene.

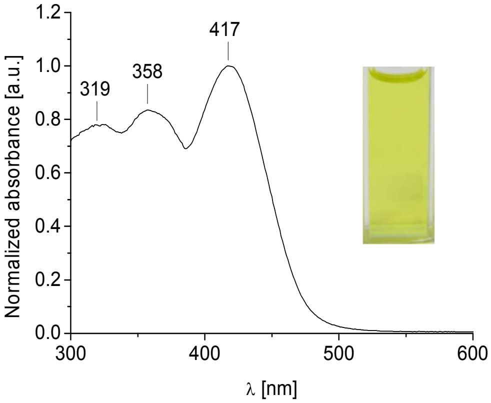

Figure 1: UV-Vis absorption spectrum and photographic image of **P1** in toluene.

P1 exhibits absorption maxima at 319 and 358 nm originating from the conjugated main chain, and another one at 417 nm originating from the conjugated ligand in the side chain. The fluorescence spectra in different solvents are shown in Fig. 2.

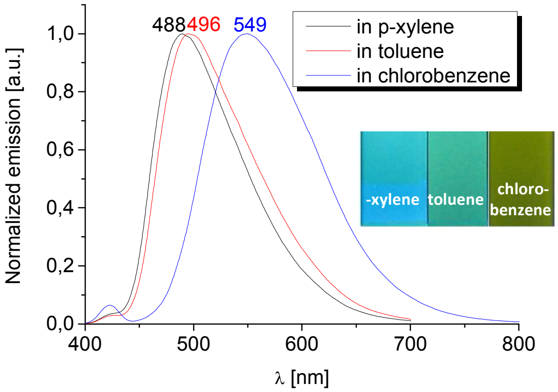

Figure 2: Fluorescence spectra and photographic images of **P1** in various solvents (λ_{exc} = 358 nm).

The emission is shifted from blue through greenish to yellow with maxima at 488, 496 and 549 nm, if either xylene, toluene or chlorobenzene are used as solvent. The solvatochromism originates from polymer-solvent interactions, in which solvent polarity, dipolarity, and the ability of the solvent to act as hydrogen bond donor or acceptor play a major role. The higher the dipolarity of the solvent, the more the absorption and fluorescence maxima are bathochromically shifted. The maxima differ by 61 nm depending on whether the non-polar p-xylene or the highly polar chlorobenzene are used as solvents. With increasing polarity of the solvent, the fluorescence quantum yield becomes lower. In p-xylene the quantum yield is 41%, in toluene and chlorobenzene 39 and 19%, respectively.

3.2 Metal ion complexation of P1 with various metal salts.

If a transition metal salt is added to the solution of **P1**, a metal ion complex is formed as indicated by a colour change of the solution from yellow to brownish red or orange. Simultanously the fluorescence of **P1** is quenched. For a quantitative analysis of the metal ion complexation a solution of **P1** was titrated with a divalent transition metal salt. For this purpose a solution of $1.43 \cdot 10^{-6}$ monomolar **P1** (monomoles = moles of repeat units) in toluene/methanol (49:1), and 1.19×10^{-3} molar transition metal salt solutions in the same solvent mixture were used. After each addition of a few drops of the metal salt solution an absorption spectrum was measured. In Fig. 3, the colour of **P1** and its various metal ion complexes in solution are shown. UV-Vis-spectra monitored during titration with $NiCl_2$, $CoCl_2$, $Fe(ClO_4)_2$, $FeCl_3$, and $MnCl_2$ are shown in the Supporting Information. (Figs. S2-S9). Colour and absorbance spectra of Fe(II) and Fe(III) complexes differ due to the formation of low- and high-spin complexes, respectively.[29]

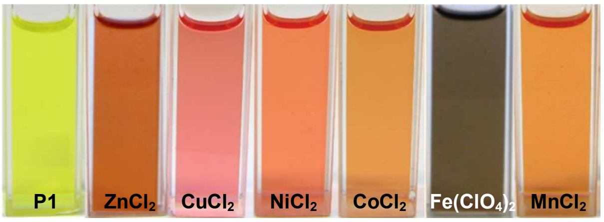

Figure 3: Photographic images of $1.43 \cdot 10^{-6}$ monomolar solutions of **P1** before and after complexation with 1 eq. of various metal salts.

The complex formation of **P1** and metal ions was studied quantitatively upon titration of a polymer solution in acetonitrile/chloroform (9:1) with a solution of zinc perchlorate in the same solvent mixture. Upon titration the low energy **π - π*** transition of the fluorene unit at 361 nm, and the **bip** absorption at 414 nm decreased. Simultaneously new bands at 390 and 506 nm appeared, which can be ascribed to a metal-to-ligand charge transfer (MLCT) band, indicating the complexation of the metal ions with the **bip**-ligands (Fig. 4 (a)). The complexation results in a colour change from yellow to orange.

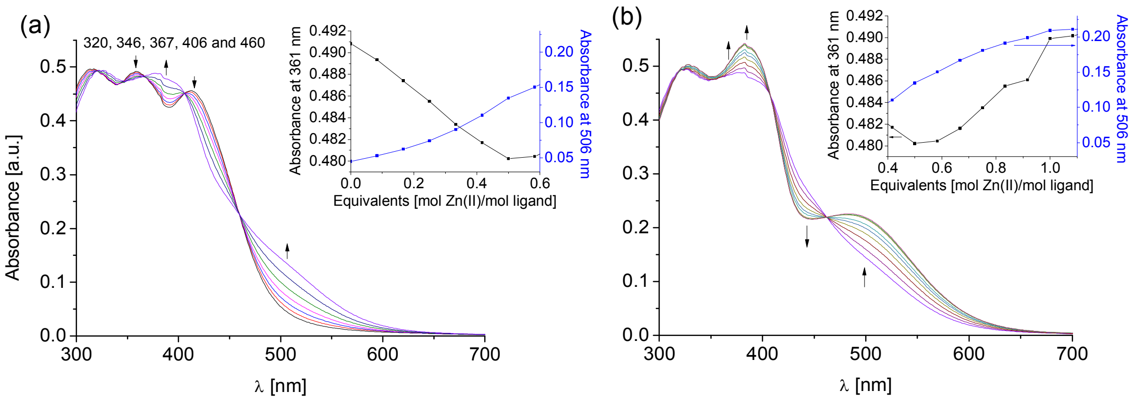

Figure 4: UV-Vis absorption spectra of **P1** (concentration: 2,54 x 10^{-5} monomol L^{-1}) in acetonitrile/chloroform 9:1 monitored before and after stepwise addition of 5 µL aliquots of zinc perchlorate solution (concentration: 2,95 x 10^{-6}) until the bis-complex (a) and the mono-complex (b) are formed. Plots of the absorbance at 361 and 506 nm vs. equivalents of Zn-ions added are shown in the insets.

With each titration step the absorbance at 361 nm decreases until 0.5 equivalents of $Zn(ClO_4)_2$ are added (see inset of Fig. 4a). This indicates the formation of the 2:1 complex (bis-complex) (see also Scheme 2). During the addition of the first 0.5 equivalents five isosbestic points at about 320, 346, 367, 406 and 460 nm occur, indicating an equilibrium between the bis-complex and the non-complexed ligands and ions. Further addition leads to formation of the mono-complexes as shown in Scheme 2. As shown in the inset of Fig. 4 (b), the formation of the mono-complex is accompanied with a re-increase of the absorbance at 361 nm until a ligand-to-metal ratio of 1:1 is reached and the mono-complex is formed. The transition from the bis- into the mono-complex is accompanied with isosbestic points at about 320, 350 and 490 nm indicating an equilibrium between the two complexes. Formation of the bis-complex and the corresponding mono-complex could only be seen for titration of **P1** with zinc perchlorate in polar solvents such as acetonitrile at 361 nm, whereas the titration with various metal chlorides, or metal perchlorate salts in non-polar solvents only led to an increase of the absorbance of the MLCT-band until the mono-complex was formed (see also Supporting Information).

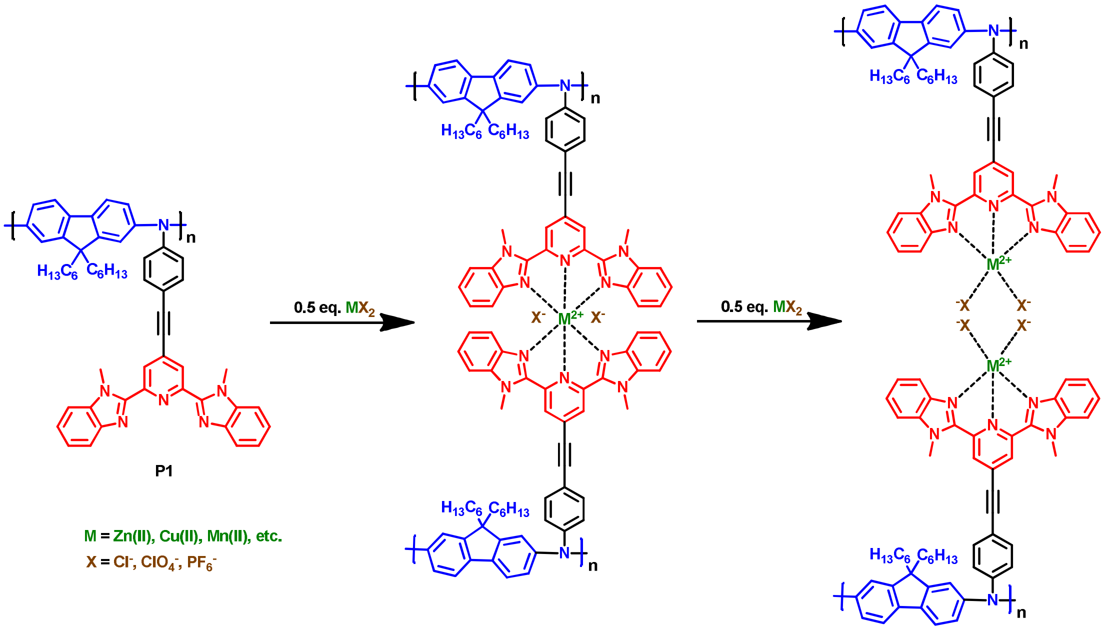

Scheme 2: Complexation of **P1** (left) with transition metal ions and formation of the bis-complex (middle) and mono-complex (right).

The formation of the bis-complex very likely proceeds as an interchain reaction and should be accompanied by cross-linking, but a precipitation was not observed. This is probably due to the low molecular weight and the low concentration of **P1** in the solution, which prevent an efficient cross-linking. Therefore the addition of metal ions only leads to formation of colloidal aggregates of the complexes. If polymer solutions with concentrations higher 0.05 mol/l were used, titration led to precipitation of the polymer-metal ion complex.

We also titrated **P1** with zinc acetate in a mixture of toluene/methanol (49:1). Again a colour change was observed due to the formation of the MLCT band. However, in this case far more of the metal salt had to be added than in case of zinc perchlorate or chloride until addition did not change the absorbance anymore (Supporting Information). The reason is that the dissociation of the metal ion complex is strongly dependent on the nature of the anion and the solvent used for the titration experiment.

3.2.2 Metal ion complexation of P1 with $CuCl_2$.

Upon titration with $CuCl_2$ in a mixture of toluene/methanol (49:1) a similar shift of the absorption bands was observed as for the titration with $ZnCl_2$. New bands occurring at 391 and 517 nm are due to formation of the MLCT complex, whereas absorption bands of the polymer at 355 and 420 nm decrease in intensity. Three isosbestic points were formed at 367, 402 and 465 nm. The complexation is accompanied by a colour change from yellow to purple. The absorption at 517 nm increased linearly until 1.0 equivalent of $CuCl_2$ was added. Additional metal ions had no further influence on the absorption spectra. UV-Vis-spectra monitored during titration with $CuCl_2$ are shown in the Supporting Information.

Fluorescence spectroscopy of the titration of **P1** with a solution of $CuCl_2$ in a 1:9 chloroform/acetonitrile solvent mixture revealed quenching of the fluorescence of **P1** upon complexation with the metal ions (Fig. 5). The emission maximum at 542 nm decreases upon addition of the metal salt until at a metal-to-ligand ratio of 0.58 the emission is fully

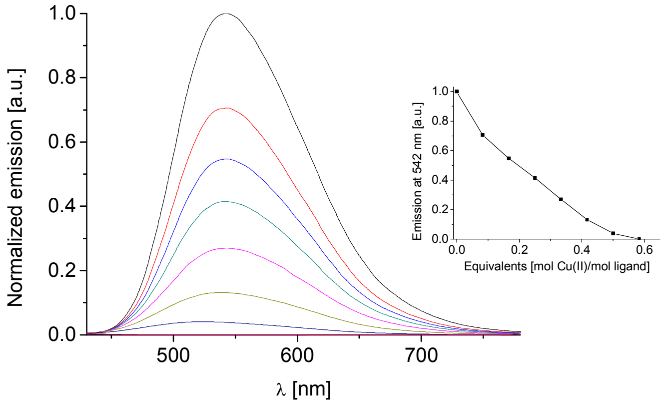

Figure 5: Fluorescence spectra of **P1** (concentration: 2,54 x 10^{-5} monomol L^{-1}) in acetonitrile/ chloroform 9:1 monitored before and after stepwise addition of 5 μL aliquots of Cu perchlorate solution (concentration: 2,95 x 10^{-6}) until the bis-complex is formed. The Inset shows the emission at 542 nm vs. equivalents of Cu-ions.

quenched. The quenching can be ascribed to the formation of the bis-complex in which an energy transfer from the conjugated system to the metal center leads to a static quenching of the fluorescence.

3.3 Coordinative layer-by-layer assembly and optical film properties.

Using coordinative layer-by-layer-assembly described in Scheme 3 films of **P1** with zinc and copper ions were deposited on pretreated quartz and ITO glass substrates.

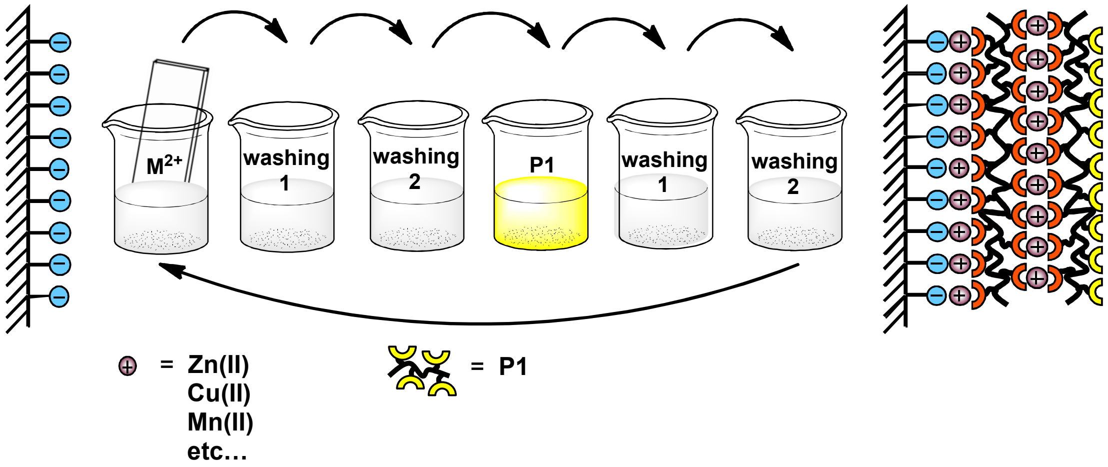

Scheme 3: Layer-by-layer-assembly of films of **P1** with various divalent transition metal ions.

PF_6^- was added to the metal salt solutions in order to decrease the solubility of the complexes, and to improve the deposition of the films. The film formation was characterized by UV-Vis-spectroscopy. Absorption spectra were recorded at intervals of two dipping cycles.

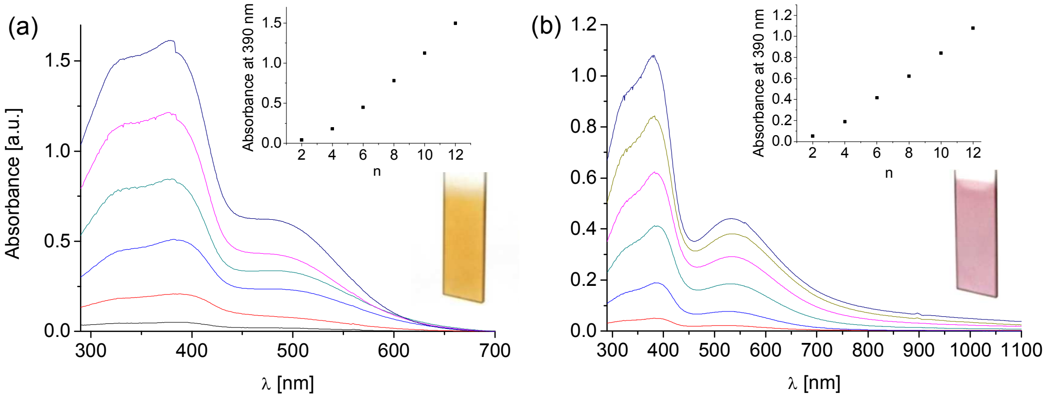

Figure 6: UV-Vis-spectra of films of **P1**/Zn(II) (a) and **P1**/Cu(II) (b) measured after *n* different numbers of dipping cycles. In the inset the absorbance at 390 nm is plotted vs. *n*. Photographic images of films with 12 double layers are also shown.

With each dipping cycle, the absorbance of the films increased. Band shape and absorption maxima of the films are in agreement with those of the zinc and copper complexes in solution. In Fig. 6 (a), absorption spectra of films of the **P1**-zinc hexafluorophosphate complex are shown. It can be seen that the absorbance of the $\pi \rightarrow \pi^*$ transition at 390 nm increases linearly with the number of deposited layers. This indicates that in each dipping cycle the same amount of polymer and metal ions are deposited. After 12 dipping cycles the film exhibits an intense orange colour and appears very homogeneous. LbL-assembly of the polymer and copper hexafluorophosphate on a quartz substrate also led to film formation (Fig. 6 (b)). A purple film with homogeneous colouration was obtained. Again the absorption increases linearly with the number of dipping cycles applied. Profilometric studies indicate that **P1**/Zn(II) films prepared upon 12 dipping cycles exhibit a thickness of 141 nm, whereas films of the **P1**-copper complex are 81 nm in thickness.

3.4 Electrochemical Properties.

In order to study the electrochemical properties, the coordination polymer films were built up on indium tin oxide(ITO)-coated glass substrates. Films of **P1** and Zn(II) or Cu(II) ions were prepared. Their cyclic voltammograms are shown in Fig. 7. Two reversible anodic waves occur, which can be related to oxidation of the nitrogen atoms of the polymer main chains (Scheme 4). All films show highly reversible oxidation steps between 0.6 and 0.9 V. The expected second wave does not always appear due to overlap with the first wave. The same is observed for the subsequent reduction. Films of **P1**/Zn(II) exhibit anodic waves at 0.40 and

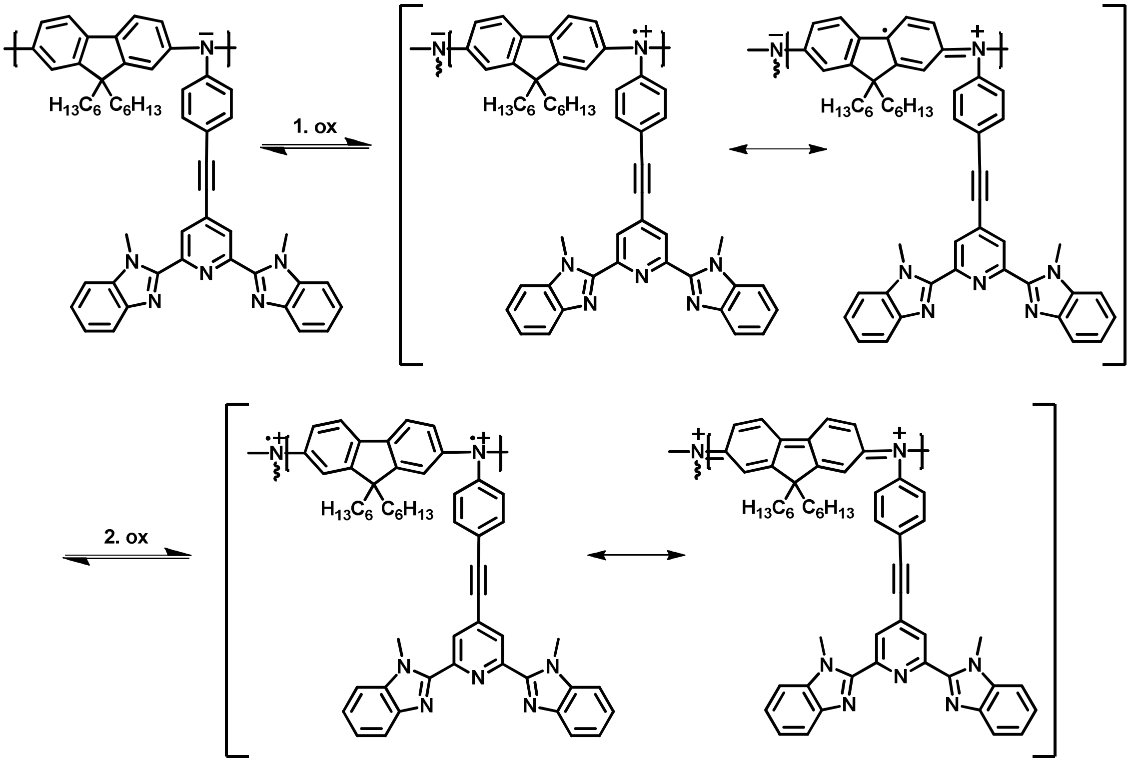

Scheme 4: Change in the conjugated π-system of **P1** upon first and second oxidation. Cation radicals, dications and quinoid structures are formed.

0.66 V. The subsequent reductive wave appears at 0.12 V. In films of **P1**/Cu(II) the two reversible anodic waves are observed at 0.44 and 0.60 V. The related reductive waves occur at 0.41 and 0.29 V.

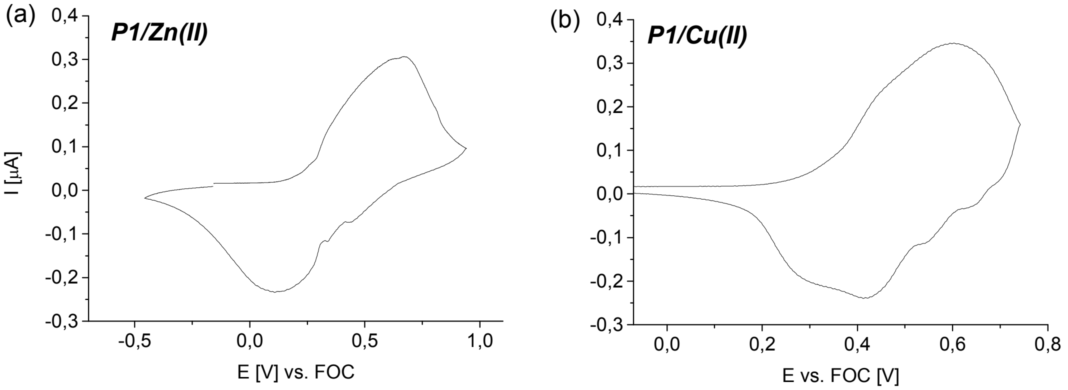

Figure 7: Cyclic voltammograms of films of **P1** and Zn(II) (a) and Cu(II) (b), (12 dipping cycles).

3.5 Electrochromic Behaviour.

Anodic oxidation and subsequent reduction of the coordination polymer films are accompanied with reversible colour changes. The change in the absorption behaviour originates from oxidation of the polymer as indicated in Scheme 4. A spectro-electrochemical study of the colour changes is shown in Fig. 8.

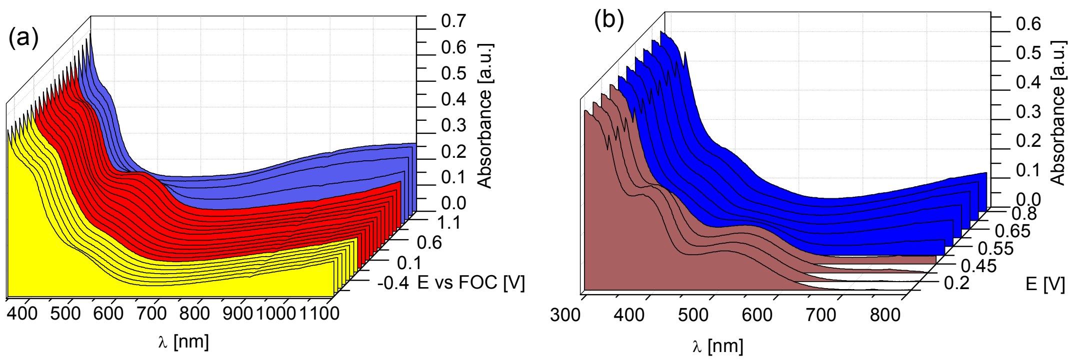

Figure 8: Spectro-electrochemical measurements of films of **P1**/Zn(II) (a) and **P1**/Cu(II) (b), (12 dipping cycles).

A conventional electrochemical three-electrode cell was used, which was placed in a UV/Vis-spectrometer. The coordination polymer film deposited on an ITO-coated glass substrate was used as working electrode. Different potentials were applied and the absorption spectra were measured. At low potential films of **P1**/Zn(II) exhibit an orange colour, which turns into red at 0.8 V, and from red to blue at 1.1 V. The first colour change originates from an increase of the absorbance at 503 nm due to formation of cation radicals in the backbone. It involves an isosbestic point at 470 nm. The second colour change goes along with a decrease of the absorbance at 503 nm and a broad increase of the absorbance from the isosbestic point at 576 nm to the infrared. It can be ascribed to formation of the dication state with a quinonoid structure in the backbone as shown in Scheme 4. Photographic images of the neutral and the fully oxidized film are shown in Fig. 9 (a).

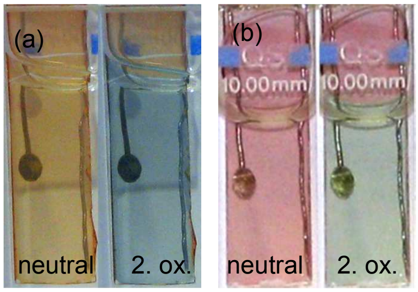

Figure 9: Photographic images of the neutral form and the second oxidation state of films of **P1** and Zn(II) (a) and Cu(II) (b), (24 dipping cycles).

Spectroelectrochemical measurements of films of **P1**/Cu(II) are shown in Fig. 8 (b). As the film in its neutral form already exhibits a reddish colour, the first oxidation has no visible effect on the absorption behaviour. The second oxidation at 0.65 V involves a colour change from purple to blue (Fig. 9 (b)), which again can be ascribed to the formation of the dipolaron state exhibiting a broad absorption ranging from 580 nm to the infrared. Simultaneously the absorption bands of the neutral chromophore at 380 and 515 nm are decreased. At a voltage above 0.5 V the isosbestic point is shifted from 612 to 580 nm.

Table 1: Physical and electrochemical properties of **P1**/metal-ion films (12 dipping cycles)

	Film thickness [nm]	Contrast [%] at 800 nm	Switching time [ms]
P1/Zn(II) film before electrochromic switching	149	53	530
P1/Zn(II) film after 40 switching cycles		35	2600
P1/Cu(II) film before electrochromic switching	81	36	320
P1/Cu(II) film after 40 switching cycles		29	800

For the **P1**/Zn(II) and **P1**/Cu(II) films we also studied switching time, contrast and long term stability. For the determination of the long term stability, the transmission at 800 nm was recorded vs. time while the films were switched between 0.0 and 0.9 V (a) and 0.0 and 0.8 V (b) every 10 seconds. The first 40 switching cycles are shown in Figs. 10 (a) and 10 (b). Switching times were determined by a linear fit of the change of absorbance as shown in Figs. 10 (c) and 10 (d). The contrast was determined from the change in transmission, Δ%T, at 800 nm obtained upon switching from the neutral to the oxidized state. The experiments were carried out with 12 double layer films (Fig. 10). The data are listed in Table 1. It turned out that the freshly prepared films exhibit switching times of 300 to 500 ms. The contrast originally is 53 %, and is reduced to about 30 % after 40 switching cycles. This may originate from partial desorption of the film from the substrate. The total reduction of the contrast was lowest for films with Cu(II) due to a stronger metal-ligand interaction than in the Zn-based film.[34,35]

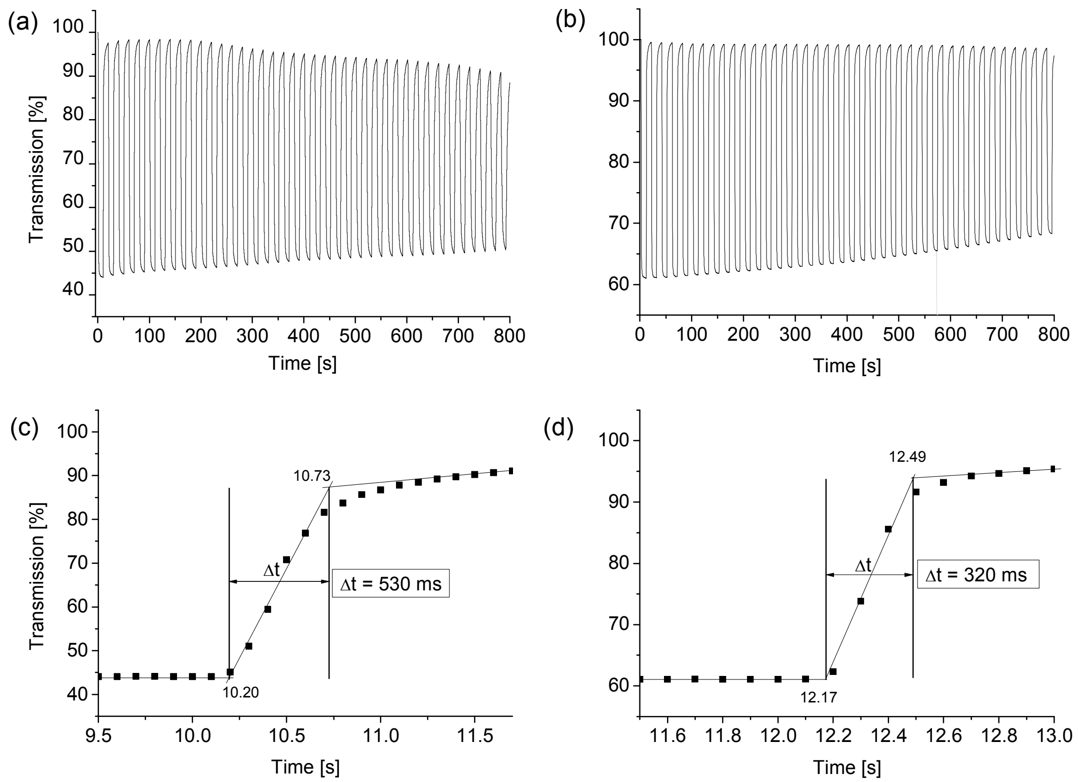

Figure 10: Electrochromic switching of films of **P1** and Zn(II) (a) and Cu(II) (b). Potential was switched between 0 and 0.9 V (a) and 0 and 0.8 V (b) while transmission was measured at 800 nm. Determination of switching times of the 1st cycle for films of **P1**/Zn(II) (c) and **P1**/Cu(II) (d), (12 dipping cycles).

3.6 Film composition and morphology.

The film morphology was studied using REM and EDX prior and subsequent to electrochromic switching. EDX measurements indicate a decrease of the carbon-to-Zn(II) ratio after several switching cycles (Fig. 11). This indicates that during the switching process the polymer is partly removed from the substrate. Removal of parts of the films could also explain the loss in contrast. REM measurements indicate that the surface of the freshly prepared films is rather homogeneous with some humps distributed over the whole

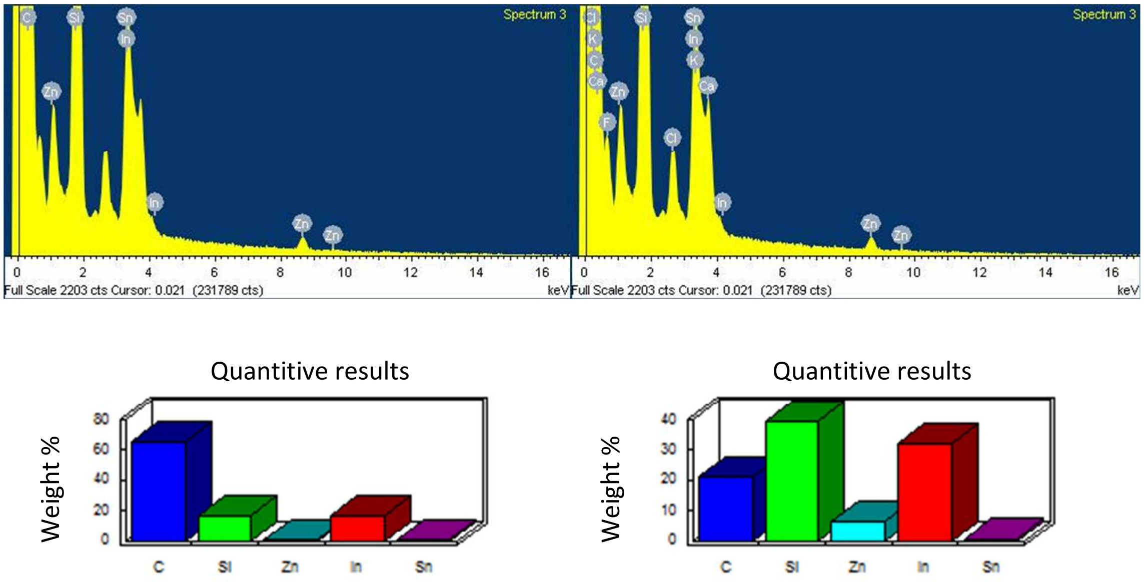

Figure 11: EDX measurements of films of **P1**/Zn(II) before (a) and after (b) electrochromic switching (up) and their quantitative results (down).

specimen (Fig. 12). After electrochemical switching the humps disappeared, but the surface generally became more inhomogeneous probably due to loss of material during the cycling process. It is especially evident at higher magnification.

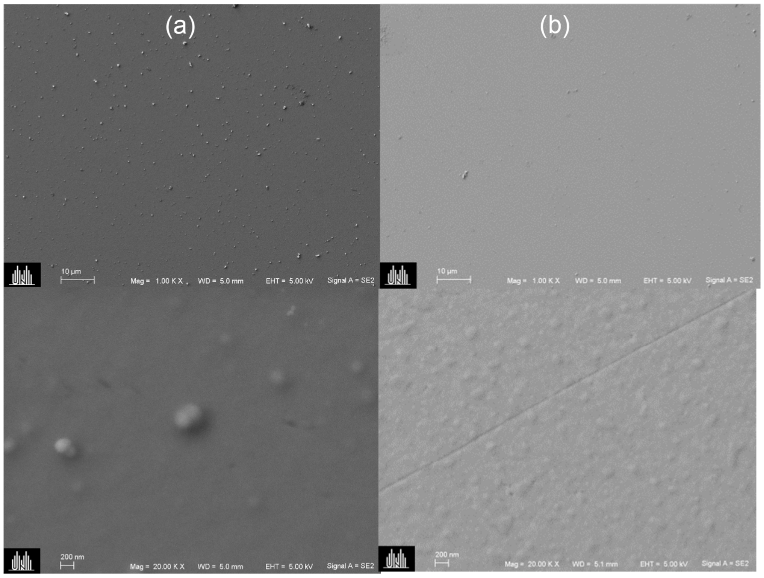

Figure 12: REM measurements of films of **P1**/Zn(II) before (a) and after (b) electrochromic switching. The upper row is shown in 1000x magnification, the lower row is shown in 5000x magnification. Pictures (a) and (b) are taken with a SE2-signal and shows the topology of the film.

4. Conclusions

First, our study indicates that a polytopic ligand **P1** with iminofluorene backbone and 2,6-bis(1′-methyl-benzimidazolyl)-pyridine (**bip**) ligand groups attached to the backbone via conjugated spacer units can be synthesized upon a palladium catalyzed amination reaction. **P1** is readily soluble in organic solvents.

Second, **P1** is able to form complexes with divalent transition metal salts such as zinc(II) and copper(II) ions in 2:1 and 1:1 stoichiometry. Metal ion complexation proceeds under noticeable colour changes from yellow to orange or purple causing a strong ionochomism of **P1**. Presence of divalent transition metal salts also quenches the photoluminescence. It is a strong effect, which can be used for sensing of transition metal ions in the ppm range.

Third, our study shows that a proper choice of solvent and nature of the counterions enables a layer-by-layer assembly of polymer-metal salt complexes on solid substrates. Ultrathin coordination polymer network films are formed upon alternating assembly of divalent transition metal salts and **P1,** similar to the assembly of transition metal salts and polyiminofluorene,[23] polycarbazolylene,[22] and polyaniline derivatives[36] with terpyridine ligands in the side chains reported recently.[22,23]

Fourth, the films are electrochromic, i.e., they exhibit reversible oxidation behaviour as well as reversible electrochromism, if the potential is switched between the neutral state at 0.0 V and the oxidized state at 0.8 V (Zn(II)) or 0.65 V (Cu(II)) vs. FOC/FOC$^+$, respectively. The colour change depends on the kind of metal ion incorporated in the films. The electrochromical properties are similar to the tpy-based coordination polymer films reported earlier,[22,23] but the different ligands and spacer units influence the metal-to-ligand charge transfer, and the strength of the ligand-to-metal ion binding leading to films of different colour and stability. On one hand, relatively thick films with high contrast and short switching times can be prepared, which is favourable for application in electrochromic devices, but on the other hand, long term stability is lower than for the **tpy** based systems[22,23] and still has to be improved. REM and EDX measurements indicate that electrochromic switching is accompanied by partial desorption. This might be due to the low molecular weight of the polymer but a weaker complex strength may also play a role. Higher molecular weights and the use of an electrolyte gel instead of a solution might help to increase the stability and maintain contrast and switching times of the films.

References

1. A. Wild, A. Winter, F. Schlütter, U. S. Schubert, *Chem. Soc. Rev.*, 2011, **40**, 1459.
2. A. S. Abd-El-Aziz, C. E. Carraher, P. D., Horvey, in *Macromolecules Containing Metal and Metal-Like Elements*, *Vol. 10: Photophysics and Photo-chemistry of Metal-Containing Polymers*, ed. Zeldin, M., John Wiley & Sons, Hoboken, N. J. 2010.
3. P. Nguyen, P. Gómes-Elipe, I. Manners *Chem. Rev.*, 1999, **99**, 1515.
4. (a) M. Rehahn, *Acta Polym.*, 1998, **49**, 201. (b) U. Velten and M. Rehahn, *Macromol. Chem. Phys*., 1998, **199**, 127.
5. T. Kaliyappan and P. Kannan, *Prog. Polym. Sci.*, 2000, **25**, 343.
6. E. C. Constable, C. E. Housecroft, J. N. Lambert, D. A. Malarek, *Chem. Commun.*, 2005, **29**, 3739.

7. X. Wang and R. McHale, *Macromol. Rapid Commun.*, 2010, **31**, 331.
8. K. A. Williams, A. J. Boydston, C. W. Bielawski, C. W. *Chem. Soc. Rev.,* 2007, **36**, 729.
9. Y.-Y. Chen, Y.-T. Tao, H.-C. Liu, *Macromolecules*, 2006, **39**, 8559.
10. D. G. Kurth, J. P. Lopez, W.-F. Dong, *Chem. Commun.,* 2005, **29**, 2119.
11. F. S. Han, M. Higuchi, D. G. Kurth, *J. Am. Chem. Soc.*, 2008, **130**, 2073.
12. O. Hagemann, M. Jorgensen, F. C. Krebs, *J. Org. Chem.*, 2006, **71**, 5546.
13. B. Tieke, *Curr. Op. Coll. Interf. Sci.*, 2011, **16**, 499.
14. D. M. Sarno, B. Jiang, D. Grosfeld, J.O. Afriyie, W. Mationzo, W. E. Jones jr., *Langmuir*, 2000, **16**, 6191.
15. H. Krass, G. Papastravou, D. G. Kurth, *Chem. Mater.*, 2003, **15**, 196.
16. W. Zhao, B. Tong, Y. Pan, J. Shen, J. Zhi, J. Shi et al., *Langmuir*, 2009, **25**, 11796.
17. N. Tuccitto, I. Delfanti, V. Torrisi, F. Scandola, C. Chiorboli, V. Stepanenko et al., *Phys. Chem. Chem. Phys.*, 2009, **11**, 4033.
18. B. Belghoul, I. Welterlich, A. Maier, A. Toutianoush, A. R. Rabindranath, B. Tieke, *Langmuir*, 2007, **23,** 5062.
19. M. Wanunu, A. Vaskevich, S. R. Cohen, H. Cohen, R. Arad-Yellin, A. Shanzer et al, *J. Am. Chem. Soc.*, 2005, **127**, 17877.
20. A. Maier, A. R. Rabindranath, B. Tieke. *Adv. Mater.*, 2009, **21**, 959.
21. I. Welterlich and B. Tieke, *Macromolecules*, 2011, **44**, 4194.
22. A. Maier, H. Fakhrnabavi, A. R. Rabindranath, B. Tieke, *J. Mater. Chem.*, 2011, **21**, 5795.
23. A. Maier, A. R. Rabindranath, B. Tieke, *Chem Mater*, 2009, **21**, 3668.
24. A. Maier, K. Cheng, J. Savich, B. Tieke, *ACS Appl. Mater. Interfaces*, 2011, **3**, 2710
25. J. B. Beck, J. M. Ineman, S. J. Rowan, *Macromolecules*, 2005, **38**, 5060.
26. J.-F. Marcoux, S. Wagaw, S. L.Buchwald, *J. Org. Chem.*, 1997, **62**, 1568.

27. F. E. Goodson, J. F. Hartwig, *Macromolecules*, 1998, **31**, 1700.

28. T. Kanbara, M. Oshima, T. Imayasu, K. Hasegawa, *Macromolecules*, 1998, **31**, 8725.

29. A. W. Addison, S. Burman, C. G. Wahlgren, O. A. Rajan, T. M. Rowe, E. Sinn, *J. Chem. Soc.*, **1987**, 2621.

30. A. R. Rabindranath, A. Maier, M. Schäfer, B. Tieke, *Macromol. Chem. Phys.*, 2009, **210**, 659.

31. S. J. Rowan and J. B. Beck, *Faraday Discuss.*, 2005, **10**, 3301.

32. J. K. Lee, G. Klaerner, R. D. Miller, *Chem. Mater.*, 1997, **11**, 11083.

33. M. Pyrasch, D. Amirbeyki, B. Tieke, *Adv. Mater.*, 2001, **12**, 1188.

34. K. Kanaizuka and H. Nishihara, in *Bottom-up Nanofabrication: Supramolecules, Self-Assemblie and Organized Films, Vol. 5 Organized Films*, Eds. K. Ariga, H. S. Nalwa American Scientific Publishers, Stevenson Ranch, 2009*,* 429.

35. R. H. Holyer, C. D. Hubbard, S. F. A. Kettle, R. G. Wilkins, *Inorg. Chem.*, 1966, **5**, 622.

36. A. Maier, B. Tieke, *J. Phys. Chem. B*, 2012, **116**, 925.

Table of contents entry

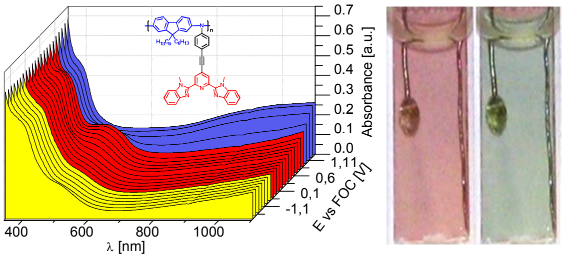

A new polyiminofluorene with conjugated bis(methylbenzimidazolyl)pyridine ligands in the side chain has been synthesized. Ionochromism of the polymer and electrochromic behaviour after coordinative layer-by-layer assembly into ultrathin films are described.